

Analysis of soil vibrations by means of the Boundary Element Method

P. Fiala, J. Granát, F. Augusztinovicz

Budapest University of Technology and Economics, Dept. of Telecommunications

Magyar tudósok körútja, 111x, Budapest, Hungary

e-mail: fiala@hit.bme.hu

Abstract

This paper introduces some results of the application of the three-dimensional Boundary Element Method for the analysis of soil vibrations. Soil is considered to be an isotropic, homogenous, linear elastic medium with known mass density, modulus of elasticity and shear. After giving the governing equations that form the base of the calculations, the paper investigates the vibrations excited by a point source on the surface of the infinite half-space, a soil layer over bedrock, and finally the effect of vertical trenches on the vibration reduction.

1 Introduction

Vibrations propagating in the soil can have undesired effects on buildings, roads or other structures. Therefore, the ability of predicting or controlling soil vibrations due to different excitation mechanisms – surface load or underground excitation – is of high importance. In order to have reliable simulation results, we must correctly describe the vibrating source, the method how the source vibrations transform to waves in the soil, how these waves propagate towards the investigated structures and transform back to structural vibrations. In this paper only the wave propagation in the soil is analyzed.

The Boundary Element Method is proven to be a very useful simulation tool in case of exterior acoustical radiation problems. Its main reason is that the excited vibrations in an infinite domain can be calculated by carrying out numerical integration only on the surface of the vibration source, so – compared to the finite element method – the computational costs can be reduced drastically. Unfortunately we cannot fully make use of this advantage in case of soil vibrations, because the infinite half-space, with which homogenous soil must be modeled, has a boundary surface of infinite size. Therefore, when dealing with soil radiations, a large surface has to be taken to account during the numerical calculations. However, the applying the Boundary Element Method seems to be one of the most efficient ways to simulate soil vibrations.

2 The mathematical model

2.1 The governing equations

Vibrations in homogenous, isotropic elastic media can be calculated from the time dependent *equation of motion*:

$$\nabla \cdot \boldsymbol{\sigma}[\mathbf{u}] = \rho \frac{\partial^2 \mathbf{u}}{\partial t^2} \quad (1)$$

In this equation $\mathbf{u} = \mathbf{u}(\mathbf{r}, t)$ denotes the displacement field, $\boldsymbol{\sigma}[\mathbf{u}] = \boldsymbol{\sigma}(\mathbf{r}, t)$ stands for the stress tensor field corresponding to \mathbf{u} , and ρ is the mass density of the elastic medium. The relationship between the stress and displacement fields is given by the *kinematical equation* (2) and *Hooke's theorem* (3):

$$\boldsymbol{\varepsilon} = \nabla \mathbf{u} + (\nabla \mathbf{u})^T \quad (2)$$

$$\boldsymbol{\sigma} = \lambda \operatorname{tr}(\boldsymbol{\varepsilon}) \mathbf{I} + 2\mu \boldsymbol{\varepsilon} \quad (3)$$

Here \mathbf{I} denotes the identity tensor, $\boldsymbol{\varepsilon}$ stands for the strain tensor and $\operatorname{tr}(\boldsymbol{\varepsilon})$ means the trace of $\boldsymbol{\varepsilon}$. λ and μ are the Lamé-constants that can be calculated from the Young-modulus (E), the shear modulus (G) or Poisson's ratio (ν) of the material:

$$\lambda = \frac{\nu E}{(1 + \nu)(1 - 2\nu)} \quad \mu = G = \frac{E}{2(1 + \nu)} \quad (4)$$

Substituting (2) and (3) to (1) leads to the *Navier–Cauchy equation* that, in case of steady state sinusoidal time variations, can be written in the form:

$$(c_p^2 - c_s^2)\nabla\nabla \cdot \mathbf{u} + c_s^2\nabla^2\mathbf{u} + \omega^2\mathbf{u} = 0 \quad (5)$$

Here ω stands for the angular frequency, c_p and c_s denote the velocities of the dilatational P- and the distortional S-waves propagating in the medium:

$$c_p = \sqrt{\frac{\lambda + 2\mu}{\rho}} \quad c_s = \sqrt{\frac{\mu}{\rho}} \quad (6)$$

To define the boundary conditions of the Navier–Cauchy equation, the investigated domain D has to be defined by giving its boundary ∂D . The boundary is split in two parts, ∂D_1 and ∂D_2 . On ∂D_1 the complex amplitudes of the displacement field vectors, on ∂D_2 that of the traction vectors must be given. The relationship between the displacement and the traction fields is defined by

$$\mathbf{t}[\mathbf{u}] = \boldsymbol{\sigma}[\mathbf{u}]\mathbf{n} \quad (7)$$

where \mathbf{n} is the outward unit normal of the boundary.

2.2 The Boundary integral equation

In order to transform the Navier–Cauchy equation to an equivalent boundary integral equation, its *Green-function* \mathbf{U} has to be used. In three-dimensional case the Navier–Cauchy equation's Green-function is [1]

$$\mathbf{U}(\mathbf{r}, \mathbf{q}) = \frac{1}{4\pi\mu} \left[\frac{e^{-jk_s r}}{r} \mathbf{I} + \frac{1}{k_s^2} \nabla\nabla \left\{ \frac{e^{-jk_s r}}{r} - \frac{e^{-jk_p r}}{r} \right\} \right] \quad (8)$$

This function describes a tensor field, and the i -th column of its matrix gives the displacement field excited by a point source in infinite medium, placed in \mathbf{q} and vibrating in the i -th coordinate direction. r denotes the distance between \mathbf{r} and \mathbf{q} , k_s and k_p are the wave numbers corresponding to c_s and c_p

$$k_s = \frac{\omega}{c_s} \quad k_p = \frac{\omega}{c_p} \quad (9)$$

Using the Green's function and *Somigliana's identity* [2], the boundary integral equation can be written in the form:

$$\oint_{\partial D} [\mathbf{U}(\mathbf{r}, \mathbf{q})] \mathbf{u}(\mathbf{r}) - \mathbf{U}(\mathbf{r}, \mathbf{q}) \mathbf{t}(\mathbf{r}) df = c\mathbf{u}(\mathbf{q}) \quad (10)$$

where the value of c is 1 for $\mathbf{q} \in D$, 0.5 for $\mathbf{q} \in \partial D$ and 0 else.

The integral equation has to be discretized using finite boundary elements and shape functions. The missing boundary displacement and traction vectors are obtained from a linear equation composed of independent discretized integral equations written for the surface points. After this, the displacement of an arbitrary point in D can be calculated by numerical integration on the boundary surface.

3 The computer code

The realized computer code was written in 2001-2002 in standard C++ language. The program handles three-dimensional boundary surfaces of arbitrary shape, discretized with rectangular or triangular finite boundary elements. It solves problems defined with both displacement- or traction-constraints and also mixed boundary conditions, and is able to make use of the multiple planar symmetry of the model in order to reduce computational time and memory used.

The numerical integration is carried out using linear shape functions and simple Gaussian quadrature formulae. The resulting linear equation is solved by means of the LU-decomposition method.

4 Analysis of soil vibrations

4.1 Soil properties

All the calculations documented in this paper were carried out using the same soil material properties. The mass density of the soil was considered to be $\rho = 2.1 \cdot 10^3 \text{ kg/m}^3$. The shear modulus and Poisson's ratio of the investigated material were $G = 53 \cdot 10^6 \text{ N/m}^2$ and $\nu = 0.19$. These values were determined by Ciesielski and Zieba [3] by seismic measurements on a test ground composed of fine and medium sands and sand-gravel mixture.

4.2 Rayleigh-waves excited by a point-source

The first very simple surface model can be seen on fig. 1. The flat truncated boundary of the infinite half-space is discretized with 60×60 square boundary elements, 7 elements per surface wave length LR. The excitation is vertical traction vector on the nodes of the four central elements and zero

traction on every other surface node. Because the excitation is simple, the calculations could be simplified by making use of the symmetry of the model and integrating only on one fourth of the boundary (shaded zone on the figure).

Fig. 2 shows the calculated displacement results for this area with an enlargement factor of $3 \cdot 10^8$, and fig. 3 describes the development of the wave amplitude with the increase of the source distance r . The fact that the wave amplitude decreases with $1/\sqrt{r}$ shows that the Rayleigh-waves propagate close to the surface, therefore the vibration energy is distributed on a cylindrical surface with finite depth.

The same important property of the Rayleigh-wave can be seen on fig. 4 which shows the wave amplitudes on the surface and on one of the vertical symmetry axes of the boundary, below the ground. This result tells that about $1.5 LR - 2 LR$ far from the ground the wave amplitude decreases by 20 dB.

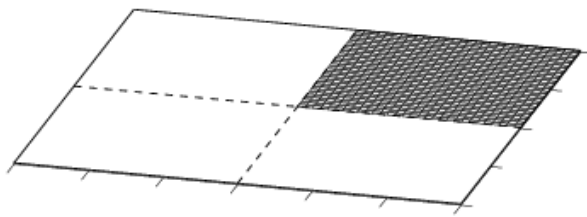


Figure 1: Truncated boundary of the half-space

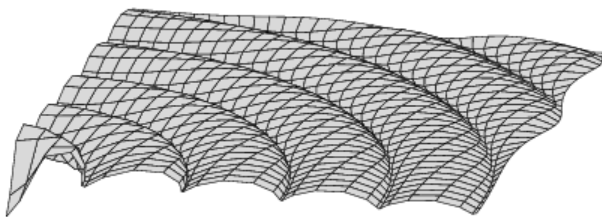


Figure 2: Rayleigh-wave excited by the point-source

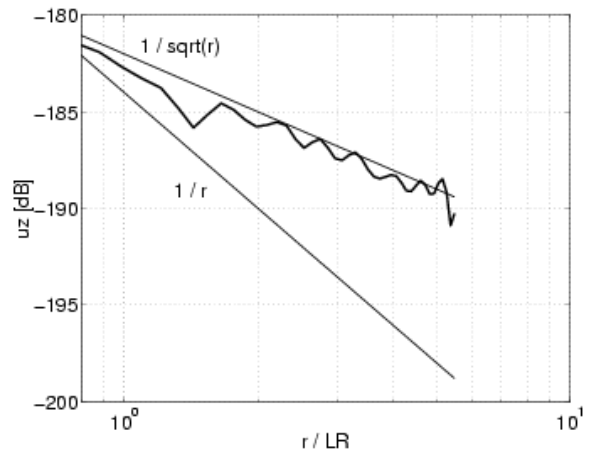


Figure 3: Attenuation of the wave amplitude

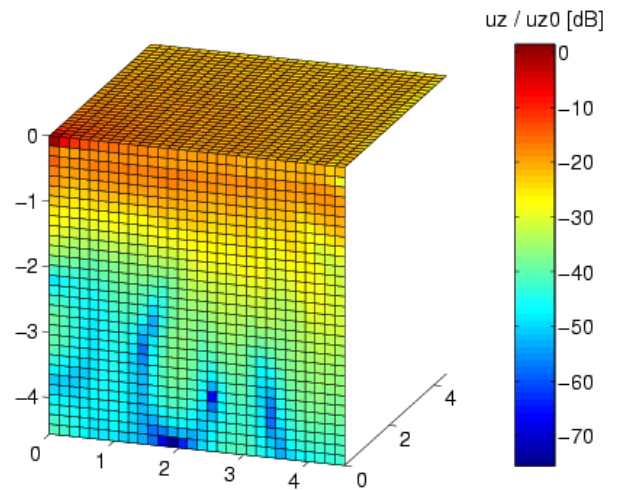


Figure 4: Attenuation of the amplitude with depth

4.3 Rayleigh-waves over bedrock

The calculations on the following model describe the behavior of a soil layer with finite depth H over rigid bedrock. The surface models that can be seen on fig. 5 consist of two parallel surfaces; one for the upper and one for the lower boundary of the soil layer. The excitation is unit vertical traction vector in the centre of the upper surface, zero traction on the other upper nodes and zero displacement on the lower surface layer. The surfaces are discretized with 50 elements along the radii and 5 symmetry planes reduce the integration domain to one thirty-second of the whole surface.

Fig. 5 shows some of the results of the calculations carried out on thirteen models with different layer width and on one with no lower layer, and the diagram of fig. 7 describes the increase of the average amplitude of the vertical u_z

and radial u_r surface wave components due to the rigid lower layer's presence.

The results show that if the layer width is less than $0.25 L_R$, then the average amplitude on the upper surface is almost 25 dB less than the amplitude due to the same excitation without the lower surface. If the layer width is greater than $1 L_R$ then the increase of both components converge to 0 dB. It is clear, because the Rayleigh wave doesn't enter the soil too deeply, and that's why a rigid layer deeper than $1.5-2 L_R$ doesn't influence the wave propagation. The computational results show, that if the layer width is between $0.5 L_R$ and $1 L_R$, then the surface amplitude can increase with up to 10 dB, which can be explained with resonance.

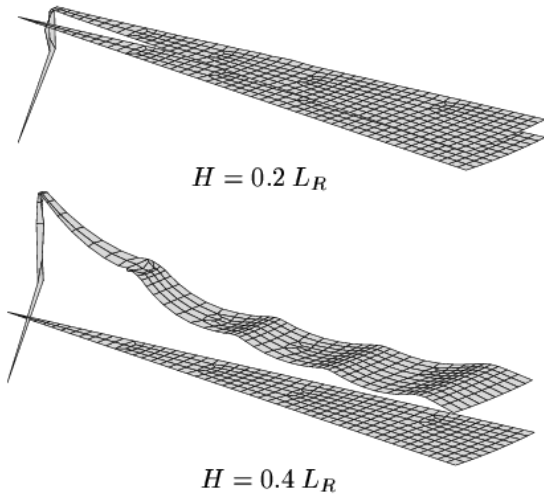


Figure 5: Surface models with different layer width

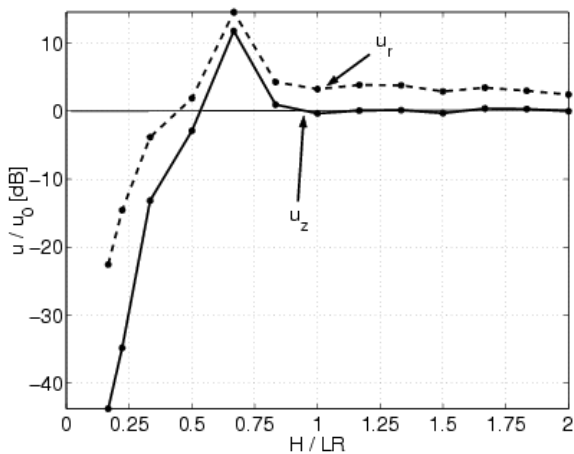


Figure 6: Increase of the average surface wave amplitude

4.4 The effects of trenches on the Rayleigh-waves

Because the Rayleigh-waves propagate near to the surface, the amplitude of these surface vibrations can be reduced by vertical trenches. Fig. 7 shows a surface model that contains not only the discretized boundary of the half-space, but also a trench that fully surrounds the central vibration source. The depth of the trench is H , and the distance of the trench from the vertical point-source is R_0 . The effect of both geometrical properties on the vibration reduction was investigated.

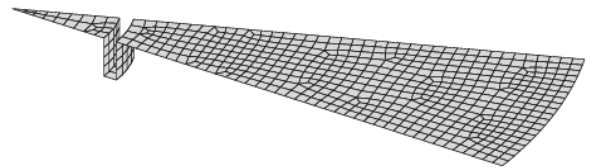


Figure 7: Truncated surface model with a trench

The diagrams on fig. 8 and fig. 9 show the vertical and radial surface wave displacement components in three different cases. In the first case (thick solid line) there is no trench around the point source, in the second case (thick dashed line) the radius of the trench is $1 L_R$ and the depth is $0.4 L_R$, while in the third case (thin solid line) the radius is $0.3 L_R$ and the depth is also $0.4 L_R$. The displacement curves show that the effect of the vibration reduction increases with the decrease of the trench radius. It also can be seen, that while the vibration amplitudes are reduced behind the trench, they can increase between the trench and the source, because the excited vibrations can interfere with those reflected from the inner side of the trench.

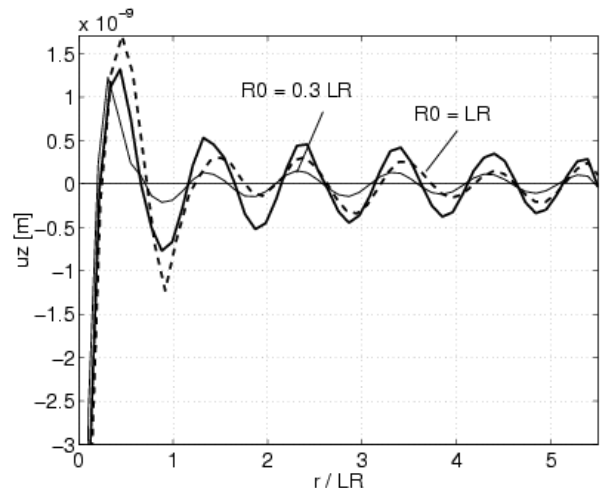


Figure 8: The vertical vibration displacements

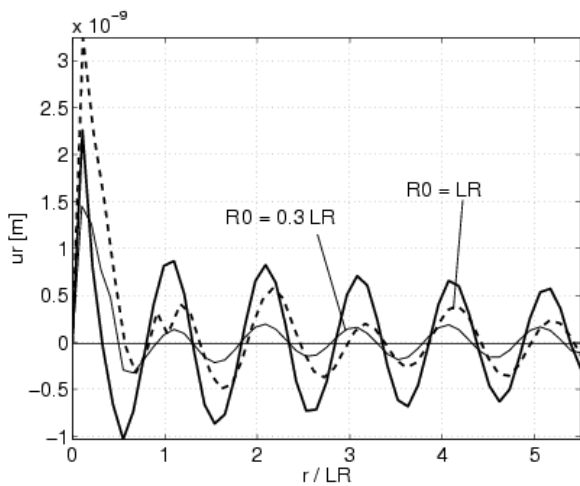


Figure 9: The radial vibration displacements

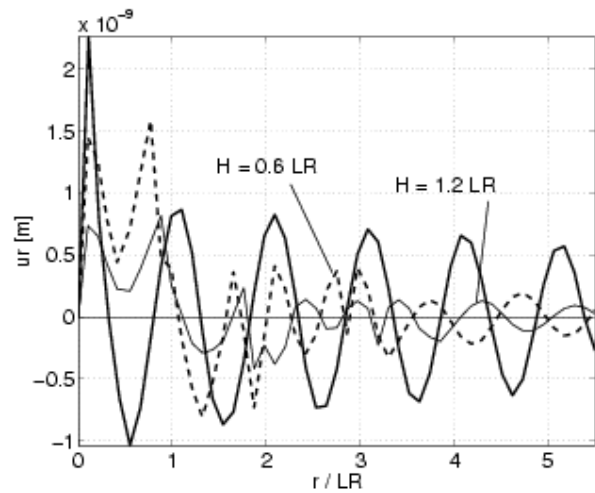


Figure 11: The radial vibration displacements

The effect of the trench depth H on the vibration reduction is shown on fig. 10 and fig. 11. As on the last diagrams, the thick line corresponds to the flat surface model, the thick dashed line describes the displacement of the vibration components in the case when the source is surrounded by a trench with radius of $0.5 LR$ and depth of $0.6 LR$. The thin solid line corresponds to depth of $1.2 LR$ and radius of $0.5 LR$. The computational results show that the increase of the trench depth increases the effect on the vibration reduction.

These diagrams are in good correlation with the measurement results of Richart, Woods and Hall [5], who stated that if the trench surrounds the source fully, then a trench depth of $0.6 LR$ is enough to reduce the vibration amplitudes to 25%, but in order to reach a reduction factor of 10%, trenches with depth smaller than $2 LR$ are not satisfactory.

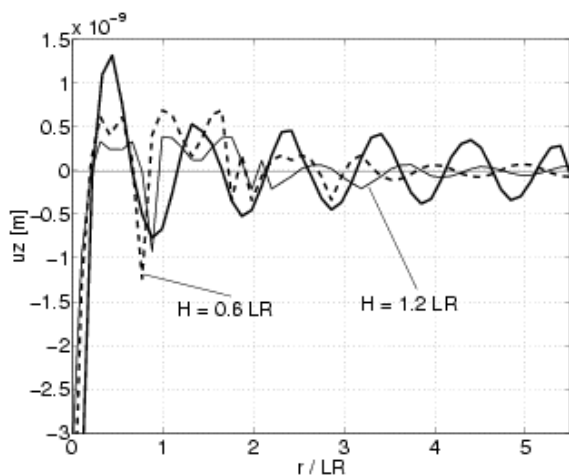


Figure 10: The radial vibration displacements

References

- [1] Y. Niwa, S. Kobayashi, M. Kithara, *Determination of eigenvalues by Boundary Element Methods*, in P. K. Banerjee, R. P. Shaw, editor, *Developments in Boundary Element Methods*, Vol. 2, Applied Science Publishers LTD., London, (1982), pp. 143-176.
- [2] J. O. Watson, Advanced implementation of the Boundary Element Method for two-and three-dimensional elastostatics, in P. K. Banerjee, R. Butterfield, editor, *Developments in Boundary Element Methods*, Vol. 1, Applied Science Publishers LTD., London, (1979), pp. 31-63.
- [3] R. Ciesielski, A. Zieba, *Experimental investigation on reduction of impact vibrations through ground by means of shallow vertical trenches*, Structural Dynamics, Krätzig et al., editors, (1990), pp. 717-722.
- [4] N. Chou, R. Le, G. Schmid, *Vibration transmitting behaviour of the soil*, Structural Dynamics, Krätzig et al., editors, (1990), pp. 701-708.
- [5] F. E. Richart, R. D. Woods, J. R. Hall, *Vibration of soils and foundations*, Prentice Hall, Inc, Englewood Cliffs, New Jersey, (1970).

